Chapter 5

BIFURCATIONS IN PRACTICAL ONE DIMENTIONAL BOOST CONVERTER

5.1 Introduction

It has been found that most feedback controlled switching circuits exhibit nonlinear phenomena and chaos over significant parts of the parameter space. It has also been revealed that in addition to saddle-node bifurcation and period-doubling cascade, the feedback controlled switching circuits exhibit many atypical bifurcation phenomena. Generally the nonlinear dynamics of physical systems are analyzed by obtaining discrete models popularly known as maps. Due to the existence of periodic clock pulses in the control logic, the Power electronic circuits like boost converters are suitable for such discrete domain modeling. We can observe the states in synchronism with the clock pulses and develop a function that maps the states from one clock instant to the next. A map is said to be smooth if it has a continuous derivative and monotonic if there is no change in the sign of the derivative. It has been found that the discrete domain modeling of most switching circuits i.e., maps are piecewise smooth and piecewise monotonic [1]. In the paper [14] the authors explored the dynamics of general piecewise smooth piecewise monotonic one dimensional (1-D) maps and apply the results in explaining the nonlinear phenomena in the boost converter without parasitic effect. The same type of analysis and application are presented in [2],[17] for two dimensional (2-D) maps. In this chapter, we explore the dynamics of piecewise smooth piecewise monotonic one dimensional (1-D) maps of Pure DC fed boost converter with parasitic effect and Rectified DC fed boost converter with parasitic effect.

5.2 Bifurcation in Piecewise smooth map:

a. The Piecewise Smooth Map

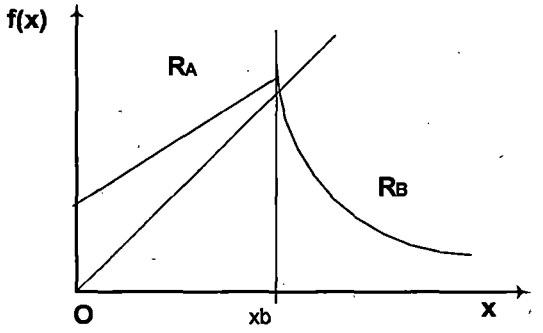

Fig. 5.1. 1-D piecewise smooth piecewise monotonic map f(x) with the border

A 1-D map f(x; μ) (fig.5.1) is considered which maps the real line R^1 to itself and depends smoothly on a parameter μ. A point x = $x_b(\mu)$ on the real line divides it into two areas R_A and R_B. The map f(x; μ) is piecewise smooth if 1) f(x; μ) is continuous in (x; μ) and 2) f(x; μ) is smooth in (x; μ) on each of the areas R_A and R_B but its derivative is discontinuous at x_b. The one-sided limits of the partial derivatives of f(x; μ) must exist at the border x_b. We require that $\frac{\delta f}{\delta x}$ can change sign only at the border x_b for piecewise monotonicity. Let the map be given by

$$f(x;\mu) = g(x;\mu), \text{ for } x \le X_b \text{ and } h(x;\mu), \text{ for } x \ge X_b \quad \ldots\ldots (5.1)$$

b. Bifurcations In The Smooth Regions

If a fixed point is in the regions either R_A or R_B, the bifurcations include the period doubling bifurcation and the saddle-node or tangent bifurcation. If $f(x;\mu_{1)=}x$ at $x_0 \neq x_b$ and $\frac{\partial}{\partial\mu} f(x;\mu) \neq 0$ and $\frac{\partial}{\partial x} f(x_0;\mu_1) = 1$ then there is a tangent bifurcation at $\mu = \mu_1$ In one side of

μ_1 there is no fixed point while in the other side of μ_1 there is one stable and one unstable fixed point. The fixed points originating in a tangent bifurcation can collide with the border with a further change of parameter. The results of such border collision bifurcation is outlined in the next sub-section. If $\frac{\partial}{\partial x} f(x_0;\mu_1) = -1$ then there is a period doubling bifurcation at $\mu = \mu_1$. In the case of piecewise monotonic maps, if a fixed point undergoes a period doubling bifurcation at μ_1 and the double-period orbit bifurcates at $\mu_2 \rangle \mu_1$ then the periodic orbit must collide with the border for some μ in $[\mu_1;\mu 2]$.

c. Border Collision Bifurcations

If the fixed point collides with the border and the parameters are changed , there is a discontinuous change in the derivative $\frac{\delta f}{\delta x}$ and the resulting phenomenon is called border collision bifurcation. Most of the bifurcations observed in power electronic circuits are of this type [1], [3],[98],[113],[114]. As the local structure of such bifurcations depends only on the local properties of the map in the neighborhood of the border, we study such bifurcations with the help of normal form: the piecewise affine approximation of f in the neighborhood of the border. The normal form is developed in the following way. We make a parameter-dependent change of coordinate by $\bar{x}$=x - x_b. The border is now given by $\bar{x} = 0$ and the map is given by $f(\bar{x} + x_b; \mu) = F(\bar{x}; \mu)$. The state space is now divided into two halves, L and R, where L = (-∞; 0] and R = [0; +∞). For simplicity, we write $F(\bar{x}; \mu)$ as F(x; μ). Suppose a fixed point of F(x; μ) is on the border when $\mu = \mu_0$, that is, F(0; μ_0) = 0. Without loss of generality, we define $\mu_0 = 0$. We expand F(x; μ) to the first order about x = μ = 0 and get

$$F(x;\mu) = ax + \mu v_A + o(x;\mu), \quad \text{for } x \le 0$$

$$F(x;\mu) = bx + \mu v_B + o(x;\mu), \quad \text{for } x \ge 0 \qquad \ldots\ldots\ldots (5.2)$$

where $$a = \lim_{x \to 0^-} \frac{\partial}{\partial x} F(x;0),$$

$$b = \lim_{x \to 0^+} \frac{\partial}{\partial x} F(x;0),$$

$$v_A = \lim_{x \to 0^-} \frac{\partial}{\partial \mu} F(x;0),$$

$$v_B = \lim_{x \to 0^+} \frac{\partial}{\partial \mu} F(x;0) \quad \ldots\ldots \qquad (5.3)$$

The continuity of the map F(x; μ) for all μ if $v_A = v_B$ and we assume this value is other than zero. v_A and v_B are eliminated from (5.2) by rescaling μ. For F(x; μ), we compute a and b, and obtain the 1-D normal form :

$$G_1(x;\mu) = ax + \mu, \quad \text{for} \quad x \le 0$$
$$= bx + \mu, \quad \text{for} \quad x \ge 0 \qquad \ldots\ldots..(5.4)$$

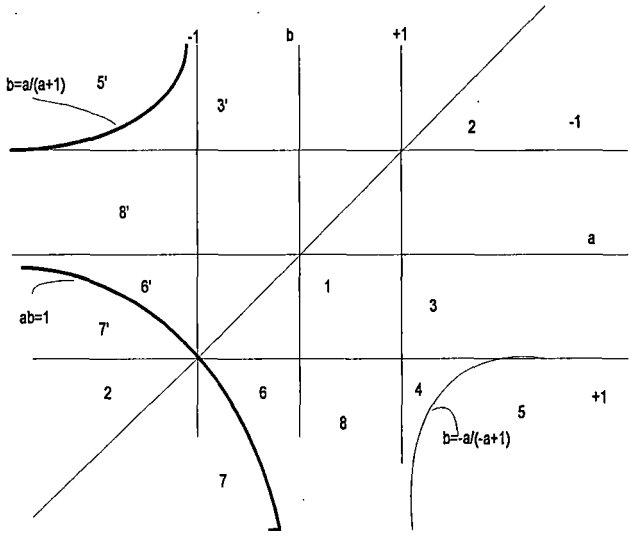

Fig. 5.2. Break up of the parameter space into regions with the same qualitative bifurcation phenomena. 1) Period-1 to Period-1; 2) No attractor to no attractor; 3) No fixed point to Period-1; 4) No fixed point to chaotic attractor; 5) No fixed point to unstable chaotic orbit (no attractor); 6) Period-1 to Period-2; 7) Period-1 to no attractor and 8) Period-1 to periodic or chaotic attractor. Primed numbers have the same bifurcation behavior as the unprimed ones when μ is varied in the reverse direction.

As μ is varied, the local bifurcation of the piecewise smooth map F(x; μ) is the same as that of the normal form G1. Various combinations of the values of a and b indicate different kinds of bifurcation behaviors as μ is varied. In Fig. 5.2, we break up the a-b parameter space into different regions with the same qualitative bifurcation phenomena.

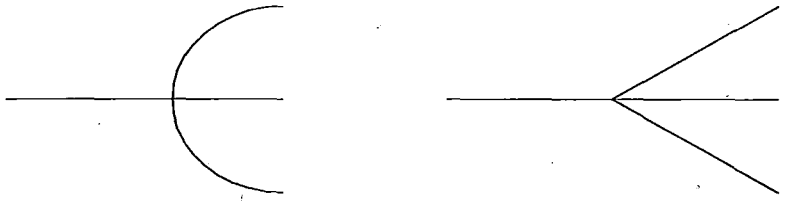

a. Standard period doubling of smooth map b. Border collision period doubling

Fig. 5.3. Bifurcation diagrams for a standard period doubling bifurcation of a smooth map and that of a border collision period doubling bifurcation of a piecewise smooth map. a. The Period-2 points diverge perpendicularly from the μ axis near the critical parameter value; b. in the second case, they may diverge at an angle that is less than 90 from the μ axis. The solid lines for attracting orbits and the dashed lines for unstable orbits.

For $\mu > 0$, all trajectories are bounded with existence of various periodic attractors and chaotic attractors. For $\mu > 0$ there can be a period adding cascade, with chaotic windows sandwiched between periodic windows, as the magnitudes of a,b are increased. It also be noted that for $\mu > 0$, the behavior is chaotic for the whole region of Case 4 and a significant portion of Case 8. The chaotic attractor of the 1-D normal form is robust in the contiguous region of the parameter space where no periodic windows exist[7]. Parameter regions are extensively studied in [4]-[6]. The current controlled boost converters are studied with respect to parameters. Regions in [8]-[10]

5.3 Boost converter with parasitic effect

a. Mathematical Modeling.

The practical boost converter (converter with parasitic effect) circuit is shown in Fig.5.4. Switching logic of the circuit is that when switch is closed the inductor current rises and

it continues till the inductor current reaches to Iref , ignoring any arriving clock pulse . As soon as the inductor current reaches to Iref , the switch is off and the inductor current falls. The switch closes again on the arrival of the next clock pulse. This is also explained by the fig.5.5.

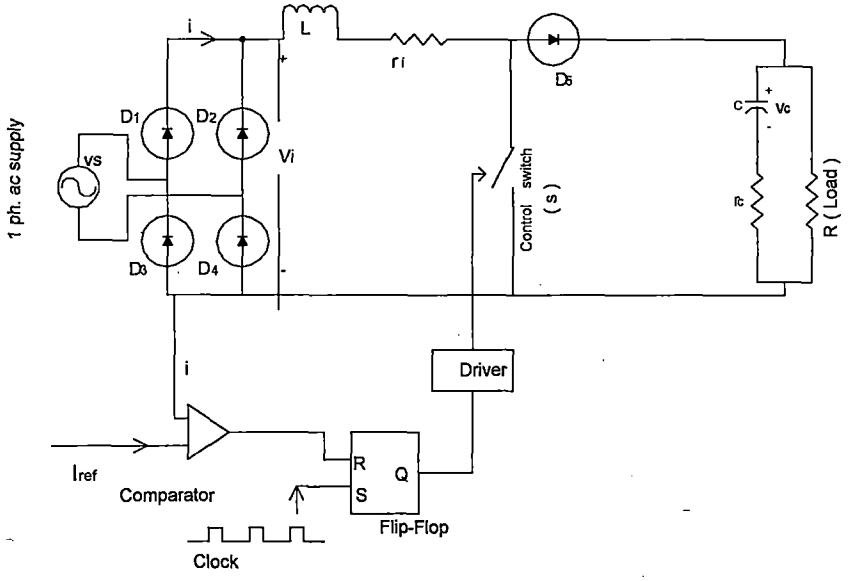

Fig. 5.4. The current mode controlled boost converter with parasitic effect and rectified DC input For pure DC input Vi is a pure DC voltage instead of a rectifier and ac input

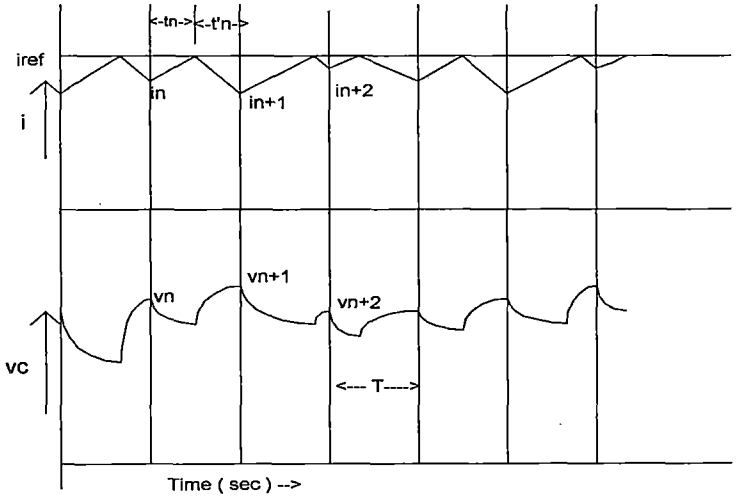

Fig. 5.5 Time plot of capacitor voltage and inductor current of the boost converter with clock pulses The circuit has two states depending on whether the control switch is opened or

closed. When switch is closed (on period) the state equations are

$$L\frac{di}{dt} = V_i - ir_i$$

$$C\frac{dv_c}{dt} = -\frac{v_c}{R + r_c} \qquad \ldots\ldots\ldots \quad (5.5)$$

and the states equations during off period (when switch is off) are

$$L\frac{di}{dt} = V_i - ir_i - i\frac{Rr_c}{R + r_c} - v_c\frac{R}{R + r_c}$$

$$C\frac{dv_c}{dt} = -\frac{v_c}{R + r_c} + i\frac{R}{R + r_c} \qquad \ldots\ldots\ldots \quad (5.6)$$

where Vi= constant for Pure DC and Vi = $|V_m Sin\omega t|$ for Rectified DC

We obtain the stroboscopic map under the following assumptions which have been adopted in a number of earlier studies [8], [9].

1) The capacitor connected in parallel with the load is large enough so that the fluctuation in the output voltage is insignificant.
2) The switching period (T) is short enough (i.e. T/RC << 1) for which he inductor current to be essentially linear during the on and off periods.

b. Bifurcations: In most practical converters the ripple amplitude is less than 1% of the output voltage and a high value of capacitance satisfies the second condition. This makes the above assumptions reasonable. Let m_1 and m_2 be the slopes of the inductor current waveform at a time during the on and off periods, respectively where L=inductance, Vo= output voltage & Vi= input voltage of the converter. The borderline between the two cases is given by the value of I_n for which the inductor current reaches I_{ref} exactly at the arrival of the next clock pulse. I_{n+1} is the next clock current value of I_n. The borderline in the state space is given by:

$$I_{border} = \left(\frac{V_i}{R}\right) + \left(I_{ref} - \left(\frac{V_i}{R}\right)\right) * e^{\frac{R}{L}T} \quad \ldots\ldots \quad (5.7)$$

The map is obtained from the equations (5.5), (5.6) and (5.7) as :

$$I_{n+1} = \left(\frac{V_i}{R}\right) + \left(I_n - \left(\frac{V_i}{R}\right)\right) * e^{-\frac{R}{L}T} \quad \text{if} \quad I_n \le I_{border} \quad \ldots\ldots \quad (5.8)$$

$$I_{n+1} = -\left(\frac{Vo}{R}\right)\left(1 - (V_i - I_n R)/(V_i - I_{ref} R)\right)e^{-\frac{R}{L}T} + \left(\frac{Vi}{R}\right) + \left(I_n - \left(\frac{V_i}{R}\right)\right)e^{-\frac{R}{L}T} \quad \text{if} \quad I_n \rangle I_{border}$$

$\ldots\ldots$ (5.9)

if $I_n > I_{border}$. The portion R_A (i.e., $i_n < I_{border}$) has slope unity, the break-point is located at (I_{border}, I_{ref}),and the portion R_B ($i_n > I_{border}$) has a slope $-m_2 / m_1$. The numerically obtained bifurcation diagram is shown in Fig. 5.6, 5.7 and 5. 8. The numerically obtained bifurcation diagram is found in [12] for pure DC fed current controlled boost converter. The parameter values are: Vi = 30 V, L = 0.1 H, T = 400 μs, Vo is varied and I_{ref} = 0.5 A. Among the diagram the fig. 5.6 already developed in [14]. fig. (5.7) is developed using the same method as in[12] with the parasitic effect To obtain fig. 5.8 input Vi is taken as rectified single phase voltage. We study the bifurcation in the system as a function of the parameter α = m2/m1. We find that there is a stable Period-1 orbit so long as α < 1. This condition of stability of the Period-1 solution (duty ratio <0:5) is well known in the theory of dc–dc converters. However, as α increases through unity, there is a period doubling bifurcation. Since R_B is linear, none of the points on R_B or their higher iterates can be stable. Therefore the fixed point moves discontinuously to the border. As the slope of R_A is unity, the resulting border collision bifurcation falls on the borderline between Cases 8 and 4. Notice that the behavior for both the regions of the parameter space is chaotic for μ > 0. Thus, there is a chaotic attractor after the border collision bifurcation. As expected, there is no periodic window for further change in the parameter. The chaotic orbit is robust. This is important from a practical point of view. It has been proposed to use chaos productively in spreading the spectrum of dc–dc converters [9], [13].

In such applications it would be necessary to ensure that the system does not come out of chaos into a periodic window due to small inadvertent change of parameters. The above observation gives a clue to designing converters with no periodic windows within the chaotic range of operation.

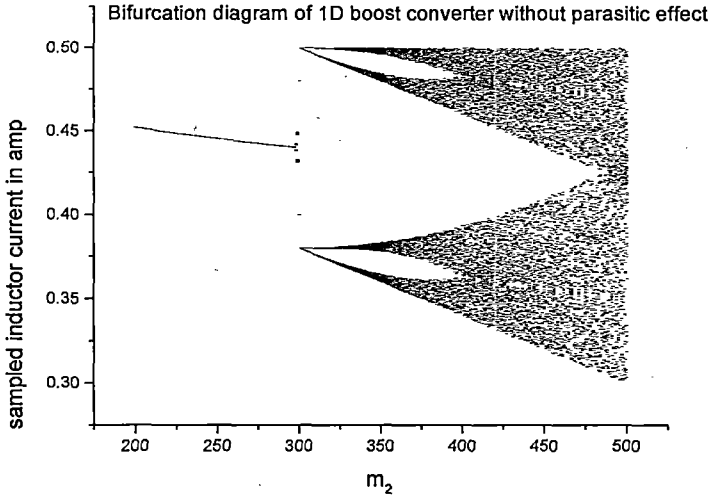

Fig.5.6. The bifurcation diagram of the current mode controlled pure DC fed boost converter without parasitic effect.

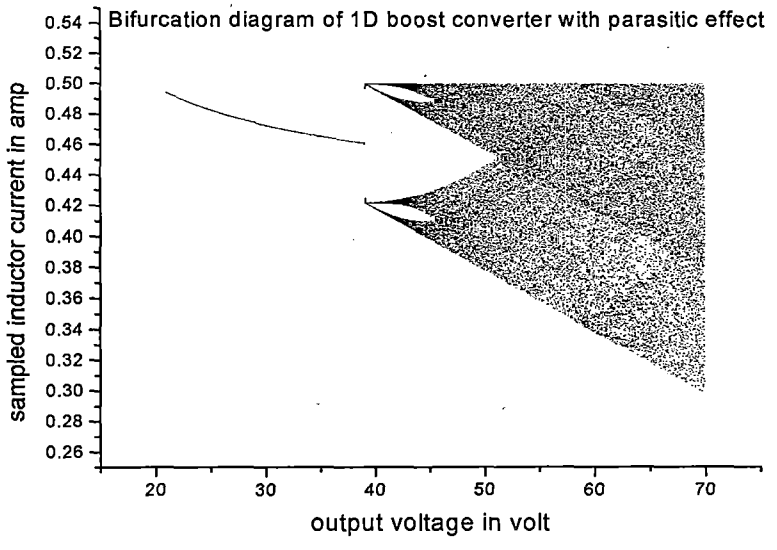

Fig.5.7. The bifurcation diagram of the current mode controlled pure DC fed boost converter with parasitic effect.

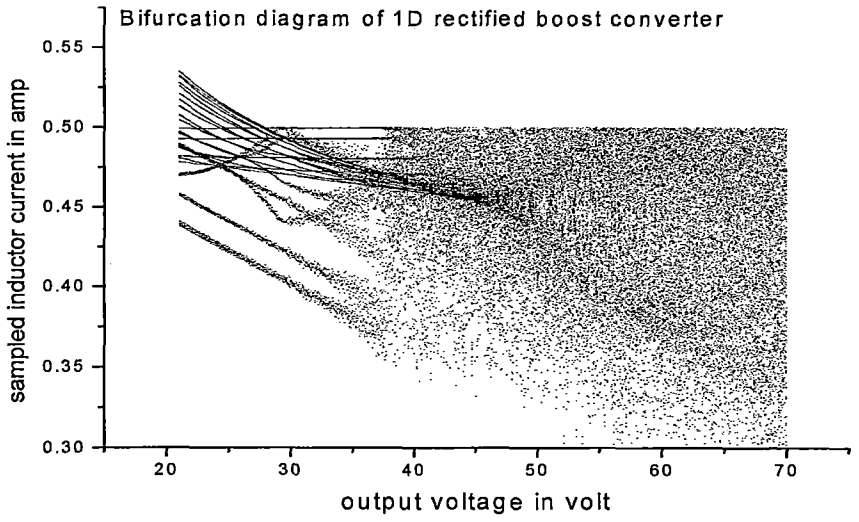

Fig.5.8. The bifurcation diagram of the current mode controlled rectified fed boost converter with parasitic effect.

5.4. Conclusions:

In this chapter we have applied the theory of bifurcations in 1-D piecewise smooth piecewise monotonic maps. We have shown that however complicated the map of a real system may be, the border collision bifurcations can be understood only in terms of its piecewise affine approximation at the border. We have developed the 1-D modeling of the boost converter with parasitic effect for two types of source voltage one for pure DC & another for Rectified DC. We presented the different Bifurcations diagram for the developed 1-D modeling which are useful in analyzing, identifying and describing the nonlinear phenomena in such circuits.

****